processes

MDPI

*Article*

# Catalytic Potential-Guided Design of Multi-Enzymatic System for DHA Production from Glycerol

**Carolina Fernández-Pizarro [1], Lorena Wilson [1] and Oscar Romero [2,*]**

[1] School of Biochemical Engineering, Pontificia Universidad Católica de Valparaíso, Valparaíso 2362803, Chile; carolina.fernandez.p@pucv.cl (C.F.-P.); lorena.wilson@pucv.cl (L.W.)
[2] Deparment of Chemical, Biological and Environmental Engineering, Universitat Autònoma de Barcelona, 08193 Cerdanyola del Vallès, Barcelona, Spain
* Correspondence: oscar.romero.ormazabal@uab.cat

**Abstract:** The growing demand for sustainable chemical production has spurred significant interest in biocatalysis. This study is framed within the biocatalytic production of 1,3-dihydroxyacetone (DHA) from glycerol, a byproduct of biodiesel manufacturing. The main goal of this study is to address the challenge of identifying the optimal operating conditions. To achieve this, catalytic potential, a lumped parameter that considers both the activity and stability of immobilized biocatalysts, was used to guide the design of a multi-enzymatic system. The multi-enzymatic system comprises glycerol dehydrogenase (GlyDH) and NADH oxidase (NOX). The enzymatic oxidation of glycerol to DHA catalyzed by GlyDH requires the cofactor NAD+. The integration of NOX into a one-pot reactor allows for the in situ regeneration of NAD+, enhancing the overall efficiency of the process. Furthermore, immobilization on $Ni^{+2}$ agarose chelated supports, combined with post-immobilization modifications (glutaraldehyde crosslinking for GlyDH), significantly improved the stability and activity of both enzymes. The catalytic potential enabled the identification of the optimal operating conditions, which were 30 °C and pH 7.5, favoring NOX stability. This work establishes a framework for the rational design and optimization of multi-enzymatic systems. It highlights the crucial interplay between individual enzyme properties and process conditions to achieve efficient and sustainable biocatalytic transformations.

**Keywords:** multi-enzymatic system; glycerol; sustainable bioprocess; dihydroxyacetone; cofactor regeneration; immobilized enzymes



**Citation:** Fernández-Pizarro, C.; Wilson, L.; Romero, O. Catalytic Potential-Guided Design of Multi-Enzymatic System for DHA Production from Glycerol. *Processes* **2024**, *12*, 2014. https://doi.org/10.3390/pr12092014

Academic Editor: Young-Seok Shon

Received: 14 August 2024
Revised: 4 September 2024
Accepted: 14 September 2024
Published: 19 September 2024



## 1. Introduction

The escalating demand for sustainable and eco-friendly chemical processes has propelled the exploration of biocatalysis as a promising alternative to traditional chemical synthesis [1,2]. The utilization of enzymes as industrial biocatalysts offers distinct advantages, such as high specificity and selectivity, mild reaction conditions, and reduced environmental impact. Among the various biocatalytic processes, the production of 1,3-dihydroxyacetone (DHA) from glycerol has received significant attention due to its wide-ranging applications in the pharmaceutical, cosmetic, and food industries [3,4].

The production of dihydroxyacetone (DHA) from glycerol, an abundant and inexpensive byproduct of biodiesel production, has garnered significant attention due to its principal use in self-tanning products [4]. Furthermore, this biotransformation aligns with the principles of a biorefinery, aiming to valorize waste streams and promote more sustainable bioprocesses.

The enzymatic oxidation of glycerol to DHA is catalyzed by glycerol dehydrogenase (GlyDH), an enzyme that requires the cofactor NAD+ for its activity [5,6]. However, the stoichiometric use of NAD+ is economically impractical, necessitating the implementation of efficient cofactor regeneration strategies [7]. NAD(P)H oxidase (NOX) has emerged as

a promising solution for cofactor regeneration, utilizing molecular oxygen as a substrate and generating water as a byproduct [8,9]. This approach offers advantages over other enzymatic methods by eliminating the need for additional organic co-substrates and their subsequent byproducts, thereby simplifying downstream processing and reducing waste generation [9]. Despite the numerous advantages of NOX-based cofactor regeneration, the availability of suitable enzymes remains a challenge. The identification and characterization of novel NOX enzymes, particularly those exhibiting high stability and activity under a broad range of pH and temperature conditions, are crucial for their successful implementation in industrial processes [9]. In this work, we used a water-forming NADH oxidase from *Streptococcus pyogenes*, a scarcely explored enzyme [8].

Enzyme immobilization has emerged as a key tool in biocatalysis, offering numerous advantages, such as enhanced enzyme stability, reusability, and simplified downstream processing [10,11]. However, the development of simple and cost-effective immobilization methods remains a significant challenge. Strategies that enable the simultaneous purification and immobilization of enzymes are particularly attractive, as they can significantly reduce the costs associated with biocatalyst preparation [12]. Furthermore, in the case of multimeric enzymes like GlyDH and NOX, preventing subunit dissociation and subsequent inactivation is crucial. It is imperative to develop immobilization strategies that not only promote the stabilization of the enzyme's quaternary structure but also enhance its overall stability [6,13]. In the context of multi-enzymatic systems, it is equally important to ensure that the chosen stabilization strategies are compatible with all the enzymes involved in the system, preserving their individual functionalities to enhance the catalytic efficiency of the whole multi-enzymatic system [14–16].

Designing multi-enzymatic systems, particularly those involving enzymes with disparate activities and stabilities, needs a comprehensive understanding of individual enzyme properties, meticulous selection of immobilization strategies, and the establishment of effective compromise conditions to balance the activity and stability of all enzymes involved [15,16]. The use of catalytic potential, a lumped parameter that considers both the activity and stability of immobilized biocatalysts, as a guide to designing a multi-enzymatic system is evaluated in this work [17]. The aim of this study is to identify compromise conditions that promote high activity and stability for all enzymes and to ensure efficient cofactor regeneration in the synthesis of DHA from glycerol.

Addressing challenges related to compromise operational conditions and enzyme stability through innovative strategies and the exploration of alternative reactor configurations can contribute to the streamlined and efficient design of multi-enzymatic systems, exemplified in this work by the GlyDH-NOX system for DHA production. Ultimately, overcoming these hurdles unlocks the full potential of biocatalysis for the sustainable and economically viable production of valuable chemicals from renewable resources.

## 2. Materials and Methods

### 2.1. Materials

Standard bead agarose 4BCL, with a size of 100 μm, was obtained by Agarose Beads Technology® (Madrid, Spain). Polyethylenimine (MO, USA). NADH and NAD+ were purchased from GERBU Biotechnik GmbH (Heidelberg, Germany). Other reagents and solvents were of the purest grade available from commercial suppliers.

### 2.2. Enzyme Production and Purification

The enzymes glycerol dehydrogenase (GlyDH) from *Geobacillus stearothermophilus* and NADH oxidase (NOX) from *Streptococcus pyogenes* were expressed in *E. coli* BL21 in high-cell-density cultures according to the methodology in [18]. The enzymes were purified by FLPC on ÄKTA pure equipment Cytiva (Marlborough, MA, USA). IMAC chromatography was employed for NOX using $Ni^{+2}$ agarose column. In the case of GlyDH, IEC chromatography was employed using an amino agarose column.

### 2.3. GlyDH Enzyme Activity Assay

GlyDH enzyme activity was obtained spectrophotometrically by following the formation of NADH ($\varepsilon_{340nm}$ = 6.22 $cm^{-1}mM^{-1}$) during glycerol oxidation. In a 1.5 mL cuvette, 25 µL of a 100 mM NAD+ solution and 1000 µL of a 100 mM glycerol solution, previously incubated at 30 °C, were added. Subsequently, 30 µL of the enzyme solution was added, at which point the reaction began. The above solutions and catalyst suspensions were prepared in 100 mM phosphate buffer with a pH of 7.0. One unit of GlyDH activity was defined as the amount of enzyme required for the formation of 1 µmol of NADH from NAD+ at pH 7.0 and 30 °C. The samples were analyzed in triplicate (n = 3), and descriptive statistics (mean and standard deviation) were used to report the yield and conversion data.

### 2.4. NOX Enzyme Activity Assay

NOX enzyme activity was obtained spectrophotometrically by following the consumption of NADH (ε340 nm = 6.22 $cm^{-1}mM^{-1}$) during its oxidation to NAD+. In a 1.5 mL cuvette, 50 µL of a 7.0 mM NADH solution and 900 µL of 100 mM phosphate buffer with a pH of 7.0, previously incubated at 30 °C, were added. Subsequently, 50 µL of the enzyme solution was added, at which point the reaction was initiated. One unit of NOX activity was defined as the amount of enzyme required for the formation of 1 µmol of NAD+ from NADH at pH 7.0 and 30 °C. The samples were analyzed in triplicate (n = 3), and descriptive statistics (mean and standard deviation) were used to report the yield and conversion data.

### 2.5. Protein Content Determination

The total protein content was determined by the Bradford method using the Coomassie® Protein Assay Reagent Kit (Thermo Scientific, Waltham, MA, USA). In a 96-well plate, 7 µL of each sample was added in 200 µL of Coomassie reagent, and the absorbance was measured after 10 min at a wavelength of 595 nm. Bovine serum albumin (BSA) was used as a protein standard.

### 2.6. Synthesis of Ag-Ni Supports

The supports were synthesized following the methodology of Mateo et al. [19] First, agarose was functionalized with epoxide groups (Ag-E) by the addition of epichlorohydrin in a basic medium and in the presence of sodium borohydride. Briefly, 1 g of Ag-E support was contacted with 10 mL of 2 M iminiodiacetic acid solution with a pH of 11 for 24 h. The support was then filtered and washed thoroughly with distilled water. The filtered support was incubated with 10 mL of 30 mg/L nickel sulfate for one hour. Finally, the support (Ag-Ni) was filtered, washed with distilled water, and stored at 4 °C.

### 2.7. Immobilization of Enzymes

The purified enzymes GlyDH and NOX were immobilized independently on nickel agarose (Ag-Ni) supports. Briefly, 1 g of support was contacted with 10 mL of enzymatic solution at pH 7.0 in 100 mM phosphate buffer at 4 °C using roller agitation. The protein loading offered for the immobilization process was 20 mg per gram of support. During the immobilization process, samples of supernatant, suspension, and enzyme solutions were taken at different times, and the activity and protein concentrations were assayed.

After immobilization, to stabilize the quaternary structure of the enzymes, the immobilized enzyme was incubated in different concentrations of glutaraldehyde (0, 0.125, 0.025, and 0.05 $v/v$) and then reduced by adding 0.5 mg of $NaBH_4$ for 30 min. Finally, the immobilized enzyme was filtered and washed with distilled water and 100 mM phosphate buffer with a pH of 7.0. For the preparation with PEI, 1 g of the immobilized enzyme was contacted with 10 mL of PEI solution (25 mg/mL) for 3 h. Then, the immobilized enzyme was filtered and washed with distilled water and 100 mM phosphate buffer with a pH of 7.0.

The metrics of immobilization were determined using the following equations:

$$Immobilization\ Yield(IY\ \%) = \frac{A_i - A_{sn}}{A_i} * 100 \quad (1)$$

$$Retained\ Activity\ (RA\ \%) = \frac{A_{sus} - A_{sn}}{A_i - A_{sn}} * 100 \quad (2)$$

$$Recovery\ Activity\ (RCA\ \%) = \frac{A_f}{A_i} * 100 \quad (3)$$

$$Immobilization\ Protein\ Yield(IYp\ \%) = \frac{P_i - P_{sn}}{P_i} * 100 \quad (4)$$

where $A_i$ is the activity offered (IU) for immobilization, $A_{sn}$ is the activity present in the supernatant (IU) at the end of immobilization, $A_{sus}$ is the activity (IU) present in the suspension at the end of immobilization, $A_f$ is the activity observed in the final catalyst (IU), $P_i$ is the protein offered (mg) for immobilization, and $P_{sn}$ is the protein present in the supernatant (mg) at the end of immobilization. The samples were analyzed in duplicate (n = 2), and descriptive statistics (mean and standard deviation) were used to report the data.

### *2.8. Stability of Biocatalyst and Determination of Catalytic Potential*

To determine the stability, 500 mg of the immobilized enzyme was incubated in 5 mL of 100 mM phosphate buffer at pH 7.5, 8.0, and 8.5 using a dry bath at temperatures of 30, 35, and 40 °C with 500 RPM agitation. The specific activity of the catalyst was monitored over time and plotted as a function of time. The resulting data were then used to fit biphasic and monophasic decay models for GlyDH (Equation (5)) and NOX (Equation (6)), respectively [20].

$$\frac{A_i}{A_0} = \left[1 + \alpha * \frac{k_{d2}}{k_{d2} - k_{d1}}\right] * e^{(-k_{d1} * t)} - \alpha * \frac{k_{d1}}{k_{d2} - k_{d1}} * e^{(-k_{d2} * t)} \quad (5)$$

$$\frac{A_i}{A_0} = e^{(-k_{d3} * t)} \quad (6)$$

$A_i/A_0$ represents the residual activity at time t, $\alpha$ is the specific activity ratio of the intermediate species with respect to the native enzyme species, and $k_{d1}$, $k_{d2}$, and $k_{d3}$ are the transition rate constants from enzyme species. The 95% confidence interval for the inactivation constants was calculated to assess the precision of the estimate.

Finally, the catalytic potential [14] was approximated using the trapezoid numerical method and implemented in MatLab R2022a.

$$CP = \int_{t_0}^{t} A_i(t)\, dt \quad (7)$$

### *2.9. Production of DHA from Glycerol in a Basket Reactor*

DHA production was conducted in a 500 mL basket reactor (Spinchem, Sweden). The reaction utilized 5.2 g of immobilized GlyDH and 1.1 g of immobilized NOX placed within the reactor's basket. The substrate consisted of 100 mM glycerol in 100 mM phosphate buffer with a pH of 7.5 at 30 °C. Samples were collected periodically, and the concentrations of glycerol and DHA were analyzed using high-performance liquid chromatography (HPLC) on an Agilent 1220 Infinity system equipped with an IC-Sep COREGEL 87H3 column. The mobile phase comprised 0.5 mM $H_2SO_4$:acetonitrile (65:35 $v/v$) at a flow rate of 0.6 mL/min, and the column's temperature was maintained at 30 °C. DHA was detected using a UV/Visible detector at 210 nm, while glycerol was detected using a Refractive Index Detector (RID). The retention times for DHA and glycerol were 12.5 min and 13.5 min, respectively. NADH quantification was performed using UV/Visible spectrophotometry

at 340 nm. Absorbance measurements were conducted on a SPECTROstar microplate reader. The samples were analyzed in triplicate (n = 3), and descriptive statistics (mean and standard deviation) were used to report the yield and conversion data.

## 3. Results and Discussions

### *3.1. Characterization of Soluble Enzymes*

Initially, pH and temperature profiles were established for each soluble enzyme to determine a working range for pH and temperature for catalytic potential analysis. Figure 1 shows that GlyDH from *G. stearothermophilus* exhibits elevated activity at an alkaline pH, peaking at pH 10. This observation aligns with reports on GlyDH from other bacteria, such as *E. coli* [21] and *G. oxydans* [22], which display maximal activity at pH 10.5 and 10, respectively. These values are notably high, considering that the average optimal pH for GlyDH typically falls between 8.0 and 9.0 [23–26]. Regarding temperature, in this study, GlyDH demonstrated peak activity between 30 °C and 40 °C. This range is lower than the average of 60 °C reported for other GlyDHs [22,24,26].

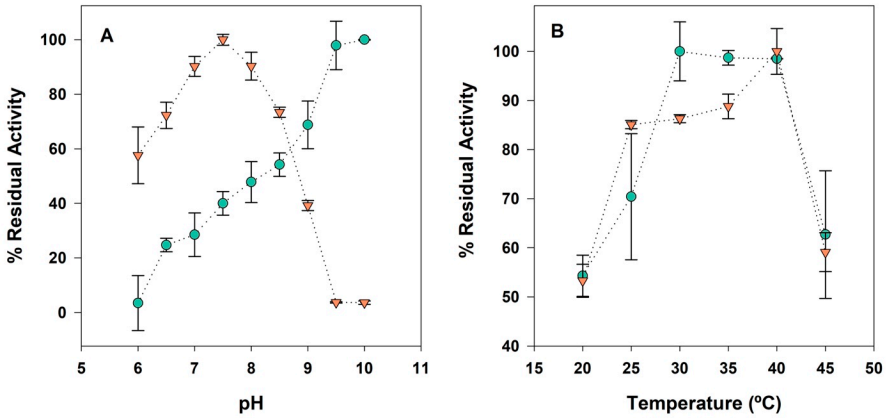


**Figure 1.** (**A**) Activity vs. pH profile for enzymes GlyDH (-●-) and NOX (-▼-) assayed in 100 mM universal Britton–Robinson buffer at 30 °C. (**B**) Activity vs. temperature profile for enzymes GlyDH (-●-) and NOX (-▼-). Error bars represent standard errors (n = 3).

On the other hand, the NOX enzyme exhibits optimal activity at pH 7.0 and 40 °C, consistent with literature reports for water-producing NADH oxidase. Non-thermophilic NOX enzymes typically exhibit an average optimal temperature of 40 °C and pH of 7.0 [8,27,28]. NOX enzymes from thermophilic microorganisms, however, exhibit optimal activity at a higher temperature of 70 °C and a slightly more alkaline pH of 7.5–8.0. Unlike the NOX from *S. pyogenes* in this study, which is a dimer, thermophilic NOX enzymes are often hexamers [8]. This multimeric structure introduces complexities such as subunit dissociation under moderate ionic strengths and challenges in immobilization, which could be considered a comparative advantage over other NOX enzymes. Furthermore, as mentioned previously, the exclusive production of $H_2O$ as a byproduct is a significant advantage of this enzyme.

Based on these results, a compromise pH range of 7.5 to 8.5 was selected for further investigation. This range favors the activity of GlyDH, which demonstrates considerably lower activity (10-fold lower) than NOX.

Regarding temperature, a range of 30 °C to 40 °C was established, encompassing the optimal activity zone for both enzymes. However, it is essential to consider that oxygen, the substrate for NOX, has limited solubility. Elevated temperatures could potentially decrease oxygen availability, thereby affecting NOX activity.

### *3.2. Immobilization of Enzymes*

The immobilization of both enzymes on $Ni^{+2}$-chelated agarose (Ag-Ni) supports was carried out. Immobilization assays were conducted at two protein concentrations: a low

loading concentration (0.5 mg/g support) and a high loading concentration (20 mg/g support) using 100 mM phosphate buffer at a pH of 7.0 and 4 °C. The immobilization kinetics are presented in Supporting Materials (Figure S1), and the final metrics for each immobilization are summarized in Table 1.

**Table 1.** Results of GlyDH and NOX enzyme immobilization on Ag-Ni support.

| Enzyme | Protein Loading (mg/g) | IYp (%) | IYact (%) | RA% | RCA% |
|---|---|---|---|---|---|
| GlyDH | 0.5 | 93.6 | 100.0 | 49.2 | 37.8 |
| GlyDH | 20 | 47.5 | 60.3 | 9.9 | 0.8 |
| NOX | 0.5 | 67.0 | 100.0 | 63.0 | 48.1 |
| NOX | 20 | 45.3 | 71.7 | 34.3 | 21.1 |

The results presented in this study demonstrate a substantial improvement in the immobilization efficiency of both enzymes compared to previous work utilizing glyoxyl-amino hetero-functional agarose supports [29]. In the prior study, recovered activities (RCA) for GlyDH and NOX were 28% and 5%, respectively. The marked increase in GlyDH activity observed here may be attributed to the inherent differences between immobilization chemistries. Immobilization via glyoxyl functional groups tends to significantly rigidify the enzyme structure, reducing the natural flexibility crucial for catalytic activity [30]. However, this increased rigidity is also associated with enhanced thermostability, a potential benefit of glyoxyl-based immobilization strategies [30]. In the case of GlyDH from *G. stearothermophilus*, an enzyme derived from a thermophilic organism that already possesses high thermostability, this benefit may not be significant [6]. Rocha et al. [31] immobilized NOX by amino functional groups, which is an irreversible immobilization process that can detach the proteins in the washing and filtering processes and does not stabilize the enzyme structure.

### *3.3. Post-Immobilization Modifications for GlyDH and NOX Catalysts*

Given the inherent challenges associated with immobilizing multimeric enzymes, such as the potential for subunit dissociation and destabilization, post-immobilization modifications were investigated to enhance the stability of both GlyDH and NOX [13]. The Ag-Ni support, even after immobilization, can contribute to the destabilization of the quaternary structure due to the presence of residual active functional groups. These free groups can interact with unbound subunits, potentially promoting enzyme movement within the support [32]. This can lead to the immobilized enzyme exhibiting lower stability than its soluble counterpart, as demonstrated by the results presented in Table 2.

**Table 2.** Results of crosslinking and coating with polymers of immobilized GlyDH.

| Type of Support and Crosslinker | RCA (%) | Specific Activity (UI/g) | $t_{1/2}$ (h) * |
|---|---|---|---|
| Soluble | - | 1.24 ** | 591 |
| Ag-$Ni^{+2}$ | 21.41 | 0.94 | 497 |
| Ag-Ni PEI | 29.53 | 0.48 | 59 |
| Ag-Ni 0.0125% Glut | 16.14 | 0.80 | 973 |
| Ag-Ni 0.025% Glut | 15.09 | 0.79 | 1036 |
| Ag-Ni 0.05% Glut | 15.58 | 0.73 | 966 |

* Half-life time incubated in 100 mM phosphate buffer at 30 °C. ** Specific activity expressed in UI/mL.

To address this issue, post-immobilization modifications were investigated, specifically focusing on coating the catalysts with polymers. Polyethyleneimine (PEI) and glutaraldehyde (Glut) were selected for their potential to prevent the dissociation of enzyme subunits. PEI, a cationic polymer, forms reversible ionic interactions with negatively charged amino acids on the protein surface, helping to maintain protein flexibility and mitigating activity loss often associated with catalyst coating. In contrast, Glut creates covalent bonds with

amino groups on the enzyme's amino acid residues, thereby rigidifying and stabilizing the enzyme structure [33]. The impact of these polymer coatings on both the activity and stability of the immobilized biocatalysts was evaluated. The half-life of the modified biocatalysts was determined at 30 °C and pH 7.5 in 100 mM phosphate buffer to assess their stability. The results of coating the enzymes with Glut and PEI are presented in Table 2.

The PEI coating led to a reduction in specific activity, activity yield, and catalyst half-life compared to the uncoated and other immobilized forms. The reversible nature of the PEI interaction, coupled with its inherent flexibility, may inadvertently promote subunit dissociation rather than stabilize the enzyme structure. Additionally, PEI could potentially chelate the zinc ion within the enzyme's active site, thereby hindering its activity. It has been reported that PEI can chelate various divalent metal ions [28]. Notably, an increase in protein yield was observed between Ag-Ni and Ag-Ni PEI, likely due to the binding of unbound proteins in the immobilization medium to the polymer upon its addition.

Crosslinking the immobilized enzyme with glutaraldehyde consistently enhanced its stability. Kumar et al. [5] immobilized an *E. coli* GlyDH in nano-reactors and observed complete activity loss in the uncrosslinked enzyme after 25 days, while the crosslinked enzyme retained 50% activity at the same time. Comparing these results to those obtained in the present study and the work of Zhang et al. [25], it can be concluded that covalent crosslinking is preferable to coating with a flexible polymer like PEI.

Furthermore, the glutaraldehyde coating experiments highlight the importance of optimizing polymer concentration. Increasing glutaraldehyde concentration from 0.025% to 0.05% led to a 70-h decrease in enzyme half-life and a 0.06 IU/g reduction in expressed activity. This decrease is likely attributable to extensive chemical modification of the enzyme at higher glutaraldehyde concentrations.

To confirm the stabilization of the quaternary structure and prevent subunit dissociation, SDS-PAGE analysis was conducted on each catalyst. The absence of a band corresponding to the enzyme subunit's molecular weight (41 kDa) in the presence of 0.05% $v/v$ Glut (see Figure S2A in Supporting Materials) suggests that this concentration is necessary to prevent the complete dissociation of the enzyme subunits.

Regarding the NOX enzyme, the same post-immobilization strategies were implemented. Table 3 reveals that immobilization via PEI coating or Glut crosslinking results in a 20% to 50% decrease in specific activity compared to uncoated catalysts, accompanied by a twofold reduction in half-life. This suggests that, in this case, crosslinking does not contribute to catalyst stabilization but rather has a detrimental effect, potentially due to the failure of crosslinking to stabilize the quaternary structure or induce the distortion of the enzyme structure. Notably, NOX immobilized on Ni-Ag exhibits a half-life twice that of the soluble enzyme.

**Table 3.** Results of crosslinking and coating with polymers of immobilized NOX.

| Type of Support and Crosslinker | RCA (%) | Specific Activity (UI/g) | $t_{1/2}$ (h) * |
|---|---|---|---|
| Soluble | - | 5.28 ** | 3.36 |
| Ag-$Ni^{+2}$ | 13.77 | 5.27 | 6.74 |
| Ag-Ni PEI | 11.07 | 2.62 | 3.7 |
| Ag-Ni 0.0125% Glut | 12.36 | 4.42 | 3.19 |
| Ag-Ni 0.025% Glut | 11.09 | 4.27 | 3.01 |
| Ag-Ni 0.05% Glut | 7.02 | 2.7 | 3.43 |

* Half-life time incubated in 100 mM phosphate buffer at 30 °C. ** Specific activity expressed in UI/mL.

Analogous to the GlyDH analysis, SDS-PAGE analysis was conducted on each NOX biocatalyst to assess the stabilization of its quaternary structure. The results indicate that NOX monomers (50 kDa) dissociate even in the presence of the highest glutaraldehyde concentration tested (see Figure S2B in Supporting Materials). This outcome aligns with previous findings, demonstrating that crosslinking does not enhance the stability of NOX.

An alternative strategy to enhance the stability of soluble NOX involves the application of reducing agents such as DTT or sodium azide [34,35]. NOX destabilization is often attributed to the oxidation of a cysteine sulfhydryl group. Consequently, the impact of DTT, a reducing agent known to prevent such oxidation, on the activity and stability of NOX immobilized on Ag-Ni was investigated. A fourfold increase in activity and a twofold increase in stability were observed at a DTT concentration of 15 mM (see Figure S3 in Supporting Materials). Similar findings have been reported for NOX from Giardia lamblia, indicating that inactivation is primarily related to overoxidation of the active site cysteine rather than denaturation [35].

To identify a suitable DTT concentration range compatible with both GlyDH and NOX, the effect of DTT concentration on their activity and stability was investigated. The results revealed a strong negative impact of DTT on GlyDH, with over 80% activity loss within just two hours of incubation with 15 mM DTT. It has been reported that reducing agents can inactivate GlyDH by reducing zinc and/or cysteine residues in the active site [36]. These results highlight the incompatibility of DTT with GlyDH, underscoring the challenges of finding compromise conditions for multi-enzyme systems.

Ultimately, for immobilized NOX, we decided to avoid any crosslinking strategy and instead pre-incubate it with 10 mM DTT prior to use to reactivate the enzyme and enhance its specific activity. For GlyDH, the biocatalyst selected was the one crosslinked with 0.025% glutaraldehyde (GlyDH-Ag-Ni-0.025% Glut).

### *3.4. Determination of Operational Compromise Conditions*

A major challenge in the design of multi-enzymatic systems is the identification of operational conditions that effectively balance the often-contrasting activity and stability profiles of the involved enzymes [14,16]. Therefore, in this study, we employed a three-level design of experiments to investigate the catalytic potential of a two-enzyme system comprising immobilized GlyDH and NOX (GlyDH-Ag-Ni-0.025% Glut and NOX-Ag-Ni, respectively). The experimental design encompassed a temperature range of 30–40 °C and a pH range of 7.5–8.5. The stability of the immobilized biocatalysts was assessed under non-reactive conditions in 100 mM phosphate buffer. The resulting inactivation kinetics are shown in Figure 2. The parameters of the decay models are shown in Supporting Materials (Table S2).

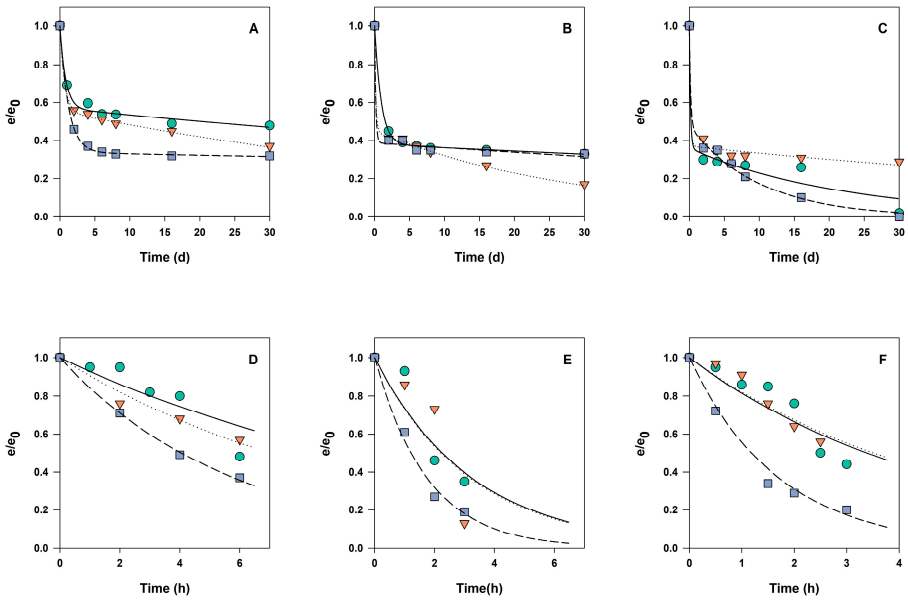


**Figure 2.** Inactivation kinetics for GlyDH-Ag-Ni-0.025% Glut at 30 °C (**A**), 35 °C (**B**), and 40 °C (**C**) and pH of 7.5 (-●-), 8.0 (··▼··), and 8.5 (--■--) and for NOX-Ag-Ni at 30 °C (**D**), 35 °C (**E**), and 40 °C (**F**) and pH of 7.5 (-●-), 8.0 (··▼··), and 8.5 (--■--).

The results presented in Figure 2 demonstrate that while GlyDH experiences an initial 40–60% activity loss within the first 48 h, it maintains a residual activity of approximately 60% for more than 30 days, even at the highest temperature tested. An analysis of its behavior across the pH range investigated reveals no significant differences in stability among the three pH values evaluated. The high thermal stability of GlyDH may be attributed to glutaraldehyde crosslinking, which stabilizes and rigidifies its structure.

In contrast to GlyDH, NOX exhibited significantly lower stability, with a 50% reduction in specific activity observed within the first 6 h under all conditions tested. At 30 °C, NOX retained 20% of its initial specific activity after 36 h, becoming completely inactivated at 54 h, regardless of pH. NOX stability decreased with increasing pH, suggesting that pH is a critical determinant of NOX stability in this system.

To identify the compromise operating conditions that balance the activity and stability of both enzymes, the response surfaces generated from the design of the experiments were analyzed. Due to the significant difference in the magnitude of the catalytic potentials between the two enzymes, the responses were normalized by dividing each value by the highest catalytic potential observed. The resulting relative catalytic potential surfaces for GlyDH and NOX are presented in Figure 3.

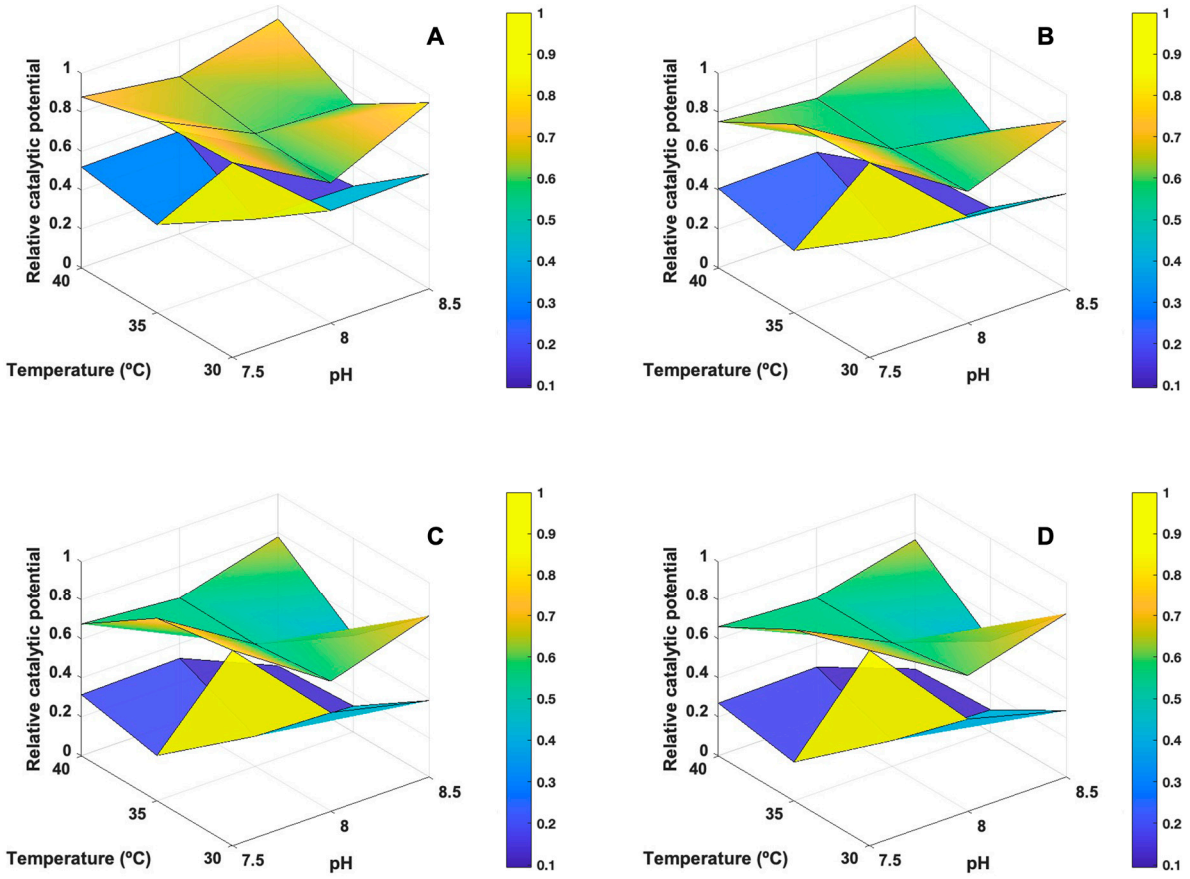


**Figure 3.** Response surface of the relative catalytic potentials of GlyDH (upper surface) and NOX (lower surface) for each temperature and pH evaluated at different times: 6 h (**A**), 12 (**B**), 24 (**C**), and 48 (**D**).

The intersection of the relative catalytic potential surfaces for GlyDH and NOX reveals the operational conditions that optimally balance the activity and stability of both enzymes. As the considered time increases from 6 to 48 h, the surfaces become increasingly distinct, with the optimal compromise point shifting towards 30 °C and pH 7.5 (Figure 3).

At 6 h, GlyDH exhibits a minimum relative catalytic potential of 72% at pH 8.0 and 30 °C, compared to its maximum potential at 30 °C and pH 7.5. This difference is less

pronounced than that observed for NOX, which shows a minimum relative potential of only 28% under its least favorable conditions. While both enzymes share the same conditions for the maximum catalytic potential, NOX emerges as the limiting factor in this system due to its lower overall stability.

The identification of optimal operating conditions in multi-enzyme systems is an ongoing challenge, with limited literature available on this specific aspect. Xu et al. [37] investigated a similar system using crosslinked enzyme aggregates (CLEAs), both individually and combined. They found that the conditions maximizing the activity of the combined CLEAs coincided with those for the CLEAs of GlyDH alone (pH 7.0 and 40 °C). However, the reported half-life of 3 h for the combined CLEAs underscores the impact of NOX instability on overall system performance, consistent with our observations. The short half-life observed by Xu et al. [37] might be attributed to the inherent instability of NOX, which acts as the limiting factor in determining the operational lifespan of the combined biocatalyst.

In light of these findings, the compromise conditions selected for the operation of the GlyDH-NOX system are 30 °C and pH 7.5, favoring the stability of the more labile NOX enzyme.

### *3.5. Production of Dihydroxyacetone from Glycerol Using the Development Multi-Enzymatic System*

To assess the applicability of the previously determined optimal compromise conditions, DHA production was conducted in a basket reactor using immobilized biocatalysts. The reaction was carried out using 100 mM glycerol and 1 mM of NADH at the compromise conditions previously established. The kinetics of the reaction are shown in Figure 4.

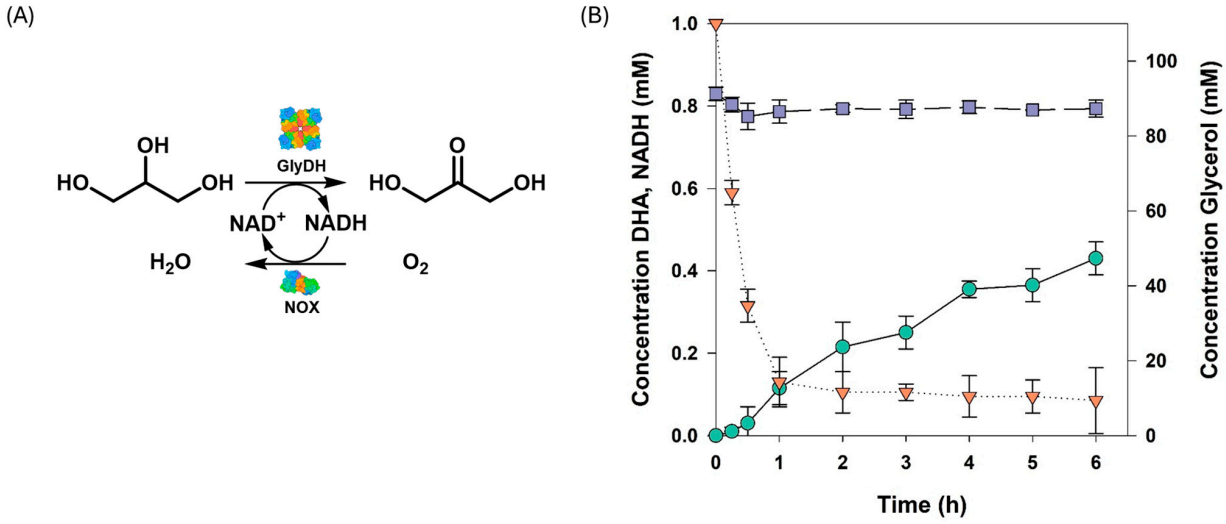


**Figure 4.** Scheme of the reaction (**A**) for the production of dihydroxyacetone from glycerol using a basket reactor and immobilized enzymes (**B**): Glycerol (■), NADH (▼), and DHA (●). The reaction was carried out at the compromise conditions of pH 7.5 and 30 °C. Error bars represent standard errors (n = 3).

Figure 4 depicts the reaction kinetics for glycerol, DHA, and NADH. The rapid consumption of NADH indicates an accumulation of the NAD+ cofactor in the reaction medium, suggesting that the reaction of glycerol oxidation is hindered by product inhibition [28]. At the end of the reaction, 98.7 mg of the product was recovered from the medium, corresponding to 87% of the DHA produced in the reaction. During the course of the reaction, DHA production reached a concentration of 0.43 mM, achieving a conversion of 3.9% and a volumetric productivity of 0.05 g $L^{-1}$ $h^{-1}$. This is consistent with previous reports on glycerol oxidation using other GlyDHs [37,38]. For instance, Xu et al. [37] reported conversions not exceeding 4.5% when using GlyDH and a cofactor regeneration

system employing recombinant NADH oxidase. The low DHA production is associated with the product inhibition of GlyDH, which slows down the reaction compared to the initial 30 min.

The results highlight the importance of achieving compromise conditions and the difficulties in coupling and optimizing a multi-enzyme system when the enzymes exhibit vastly different activities and stabilities [16,39]. Additionally, a limitation of this multi-enzyme system is the strong substrate inhibition experienced by GlyDH. Further improvement of the multi-enzyme system should address this issue through protein engineering of GlyDH or process strategies such as in situ product removal [40].

## 4. Conclusions

In this study, we successfully developed an efficient multi-enzymatic system for DHA production from glycerol, addressing the challenges associated with balancing the activity and stability of enzymes by selecting the compromise operational conditions based on the catalytic potential. The immobilization of GlyDH and NOX on $Ni^{+2}$ agarose chelated supports, coupled with post-immobilization modifications, significantly enhanced their stability and activity. The use of glutaraldehyde crosslinking proved particularly effective in stabilizing GlyDH. Based on the analysis of catalytic potential, the compromise conditions were identified as 30 °C and pH 7.5, favoring NOX stability. Although the final DHA yield was limited by product inhibition, this study provides valuable insights into the design and optimization of multi-enzymatic systems for biocatalytic processes, paving the way for the sustainable production of valuable chemicals from renewable resources. Future research should focus on addressing product inhibition and exploring alternative reactor configurations to further enhance the efficiency and productivity of this promising biocatalytic system.

**Supplementary Materials:** The following supporting information can be downloaded at: https://www.mdpi.com/article/10.3390/pr12092014/s1, Figure S1. Immobilization kinetics for GlyDH and NOX enzymes on Ag-$Ni^{+2}$ support; Figure S2. SDS-PAGE analysis of immobilized GlyDH and NOX biocatalyst crosslinked with glutaraldehyde; Figure S3. Half-life and activity of soluble NOX in the presence of different concentrations of DTT; Table S1. Effect of DTT on the stability of GlyDH. Table S2. Inactivation parameters and catalytic potential of GlyDH and NOX incubated at different temperatures and pH.

**Author Contributions:** Conceptualization, O.R. and L.W.; methodology, C.F.-P., O.R. and L.W.; formal analysis, C.F.-P., O.R. and L.W.; investigation, C.F.-P.; resources, O.R. and L.W.; data curation, C.F.-P. and L.W.; writing—original draft preparation, C.F.-P.; writing—review and editing, O.R. and L.W.; visualization, C.F.-P.; supervision, O.R. and L.W.; project administration, O.R. and L.W.; and funding acquisition, O.R and L.W. All authors have read and agreed to the published version of the manuscript.

**Funding:** This work was financed by the Chilean Fondecyt Grant 3170258 (ANID, Chile). C.P. acknowledges the financial support of Beca exención arancel 2019 PUCV, Beca ANID de doctorado nacional (21201788).

**Data Availability Statement:** The data presented in this study are available upon request from the corresponding author.

**Acknowledgments:** The authors would like to thank Javier Rocha-Martin from Universidad Complutense of Madrid, Spain and Jose Luis Garcia from Centro de Investigaciones Biológicas Margarita Salas, CSIC, Madrid, Spain for the kind donation of the *E. coli* strains for the production of GlyDH and NOX, respectively.

**Conflicts of Interest:** The authors declare no conflicts of interest.

## References

1. Alcántara, A.R.; Domínguez de María, P.; Littlechild, J.A.; Schürmann, M.; Sheldon, R.A.; Wohlgemuth, R. Biocatalysis as Key to Sustainable Industrial Chemistry. *ChemSusChem* **2022**, *15*, e202102709. [CrossRef] [PubMed]
2. Woodley, J.M. New frontiers in biocatalysis for sustainable synthesis. *Curr. Opin. Green. Sustain. Chem.* **2020**, *21*, 22–26. [CrossRef]

3. Ripoll, M.; Betancor, L. Opportunities for the valorization of industrial glycerol via biotransformations. *Curr. Opin. Green Sustain. Chem.* **2021**, *28*, 100430. [CrossRef]
4. Ciriminna, R.; Fidalgo, A.; Ilharco, L.M.; Pagliaro, M. Dihydroxyacetone: An updated insight into an important bioproduct. *Chemistryopen* **2018**, *7*, 233–236. [CrossRef] [PubMed]
5. Kumar, G.S.; Wee, Y.; Lee, I.; Sun, H.J.; Zhao, X.; Xia, S.; Kim, S.; Lee, J.; Wang, P.; Kim, J. Stabilized glycerol dehydrogenase for the conversion of glycerol to dihydroxyacetone. *J. Chem. Eng.* **2015**, *276*, 283–288. [CrossRef]
6. Rocha-Martin, J.; Acosta, A.; Berenguer, J.; Guisan, J.M.; Lopez-Gallego, F. Selective oxidation of glycerol to 1,3-dihydroxyacetone by covalently immobilized glycerol dehydrogenases with higher stability and lower product inhibition. *Bioresour. Technol.* **2014**, *170*, 445–453. [CrossRef] [PubMed]
7. Mordhorst, S.; Andexer, J.N. Round, round we go-strategies for enzymatic cofactor regeneration. *Nat. Prod. Rep.* **2020**, *37*, 1316–1333. [CrossRef]
8. Gao, H.; Tiwari, M.K.; Kang, Y.C.; Lee, J.K. Characterization of $H_2O$-forming NADH oxidase from *Streptococcus pyogenes* and its application in l-rare sugar production. *Bioorg. Med. Chem. Lett.* **2012**, *22*, 1931–1935. [CrossRef]
9. Rehn, G.; Pedersen, A.T.; Woodley, J.M. Application of NAD(P)H oxidase for cofactor regeneration in dehydrogenase catalyzed oxidations. *J. Mol. Catal. B Enzym.* **2016**, *134*, 331–339. [CrossRef]
10. Wilson, L.; Illanes, A.; Romero, O.; Ottone, C. Chapter 17—Future Perspectives in Enzyme Immobilization. In *Biocatalyst Immobilization*; Ferreira, M.L., Ed.; Academic Press: New York, NY, USA, 2023.
11. Ottone, C.; Romero, O.; Urrutia, P.; Bernal, C.; Illanes, A.; Wilson, L. Enzyme Biocatalysis and Sustainability. In *Nanostructured Catalysts for Environmental Applications*; Piumetti, M., Bensaid, S., Eds.; Springer International Publishing: Berlin/Heidelberg, Germany, 2021; pp. 383–413.
12. Ardao, I.; Benaiges, M.D.; Caminal, G.; Alvaro, G. One step purification-immobilization of fuculose-1-phosphate aldolase, a class II DHAP dependent aldolase, by using metal-chelate supports. *Enzyme Microb. Technol.* **2006**, *39*, 22–27. [CrossRef]
13. Fernandez-Lafuente, R. Stabilization of multimeric enzymes: Strategies to prevent subunit dissociation. *Enzyme Microb. Technol.* **2009**, *45*, 405–418. [CrossRef]
14. Illanes, A.; Wilson, L. Parameters for the Evaluation of Immobilized Enzymes Under Process Conditions. In *Immobilization of Enzymes and Cells: Methods and Protocols*; Guisan, J.M., Bolivar, J.M., López-Gallego, F., Rocha-Martín, J., Eds.; Springer: New York, NY, USA, 2020; pp. 65–81.
15. Silva, P.; Illanes, A.; Wilson, L.; Conejeros, R. One-pot Heterogeneous Biocatalysis under Thermal Decay for Fructose Production from Lactose using Co-Immobilized Enzymes: Modeling and Simulation. *ChemCatChem* **2024**, *16*, e202301240. [CrossRef]
16. Wilson, L.; Illanes, A.; Ottone, C.; Romero, O. Co-immobilized carrier-free enzymes for lactose upgrading. *Curr. Opin. Green Sustain. Chem.* **2022**, *33*, 100553. [CrossRef]
17. Urrutia, P.; Mateo, C.; Guisan, J.M.; Wilson, L.; Illanes, A. Immobilization of *Bacillus circulans* β-galactosidase and its application in the synthesis of galacto-oligosaccharides under repeated-batch operation. *Biochem. Eng. J.* **2013**, *77*, 41–48. [CrossRef]
18. Calleja, D.; Kavanagh, J.; De Mas, C.; Lopez-Sants, J. An engineering approach; Simulation and prediction of protein production in fed-batch *E. coli cultures:* An. engineering approach. *Biotechnol. Bioeng.* **2016**, *113*, 772–782. [CrossRef] [PubMed]
19. Mateo, C.; Bolivar, J.M.; Godoy, C.A.; Rocha-Martin, J.; Pessela, B.C.; Curiel, J.A.; Muñoz, R.; Guisan, J.M.; Fernández-Lorente, G. Improvement of enzyme properties with a two-step immobilizaton process on novel heterofunctional supports. *Biomacromolecules* **2010**, *11*, 3112–3117. [CrossRef]
20. Henley, J.P.; Sadana, A. Deactivation Theory. *Biotechnol. Bioeng.* **1986**, *28*, 1277–1285. [CrossRef]
21. Piattoni, C.V.; Figueroa, C.M.; Diez, M.D.; Parcerisa, I.L.; Antuña, S.; Comelli, R.A.; Guerrero, S.A.; Beccaria, A.J.; Iglesias, A.Á. Production and characterization of Escherichia coli glycerol dehydrogenase as a tool for glycerol recycling. *Process Biochem.* **2013**, *48*, 406–412. [CrossRef]
22. Richter, N.; Neumann, M.; Liese, A.; Wohlgemuth, R.; Eggert, T.; Hummel, W. Characterisation of a recombinant NADP-dependent glycerol dehydrogenase from *Gluconobacter oxydans* and its application in the production of L-glyceraldehyde. *ChemBioChem* **2009**, *10*, 1888–1896. [CrossRef]
23. Chauliac, D.; Wang, Q.; St John, F.J.; Jones, G.; Hurlbert, J.C.; Ingram, L.O.; Shanmugam, K.T. Kinetic characterization and structure analysis of an altered polyol dehydrogenase with d-lactate dehydrogenase activity. *Protein Sci.* **2020**, *29*, 2387–2397. [CrossRef]
24. Ko, G.S.; Nguyen, Q.T.; Kim, D.H.; Yang, J.K. Biochemical and molecular characterization of glycerol dehydrogenase from *klebsiella pneumoniae*. *J. Microbiol. Biotechnol.* **2020**, *30*, 271–278. [CrossRef] [PubMed]
25. Wang, L.; Wang, J.; Shi, H.; Gu, H.; Zhang, Y.; Li, X.; Wang, F. Characterization of glycerol dehydrogenase from *thermoanaerobacterium thermosaccharolyticum* DSM 571 and GGG motif identification. *J. Microbiol. Biotechnol.* **2016**, *26*, 1077–1086. [CrossRef] [PubMed]
26. Fan, J.; Zhang, Z.; Long, C.; He, B.; Hu, Z.; Jiang, C.; Zeng, B. Identification and functional characterization of glycerol dehydrogenase reveal the role in kojic acid synthesis in *Aspergillus oryzae*. *World J. Microbiol. Biotechnol.* **2020**, *36*, 136. [CrossRef] [PubMed]
27. Li, F.L.; Shi, Y.; Zhang, J.X.; Gao, J.; Zhang, Y.W. Cloning, expression, characterization and homology modeling of a novel water-forming NADH oxidase from *Streptococcus mutans* ATCC 25175. *Int. J. Biol. Macromol.* **2018**, *113*, 1073–1079. [CrossRef]

28. Zhang, J.D.; Cui, Z.M.; Fan, X.J.; Wu, H.L.; Chang, H.H. Cloning and characterization of two distinct water-forming NADH oxidases from *Lactobacillus pentosus* for the regeneration of NAD. *Bioprocess. Biosyst. Eng.* **2016**, *39*, 603–611. [CrossRef]
29. Rocha-Martin, J.; Acosta, A.; Guisan, J.M.; López-Gallego, F. Immobilizing systems biocatalysis for the selective oxidation of glycerol coupled to in situ cofactor recycling and hydrogen peroxide elimination. *ChemCatChem* **2015**, *7*, 1939–1947. [CrossRef]
30. Mateo, C.; Palomo, J.M.; Fuentes, M.; Betancor, L.; Grazu, V.; López-Gallego, F.; Pessela, B.C.; Hidalgo, A.; Fernández-Lorente, G.; Fernández-Lafuente, R.; et al. Glyoxyl agarose: A fully inert and hydrophilic support for immobilization and high stabilization of proteins. *Enzyme Microb. Technol.* **2006**, *39*, 274–280. [CrossRef]
31. Rocha-Martín, J.; Rivas, B.d.l.; Muñoz, R.; Guisán, J.M.; López-Gallego, F. Rational Co-Immobilization of Bi-Enzyme Cascades on Porous Supports and Their Applications in Bio-Redox Reactions with In Situ Recycling of Soluble Cofactors. *ChemCatChem* **2012**, *4*, 1279–1288. [CrossRef]
32. Diamanti, E.; Arana-Peña, S.; Ramos-Cabrer, P.; Comino, N.; Carballares, D.; Fernandez-Lafuente, R.; López-Gallego, F. Intraparticle Macromolecular Migration Alters the Structure and Function of Proteins Reversibly Immobilized on Porous Microbeads. *Adv. Mater. Interfaces* **2022**, *9*, 2200263. [CrossRef]
33. Barbosa, O.; Ortiz, C.; Berenguer-Murcia, Á.; Torres, R.; Rodrigues, R.C.; Fernandez-Lafuente, R. Glutaraldehyde in bio-catalysts design: A useful crosslinker and a versatile tool in enzyme immobilization. *RSC Adv.* **2014**, *4*, 1583–1600. [CrossRef]
34. Claiborne, A.L.; Miller, H.; Parsonage, D.; Ross, R.P. Protein-sulfenic acid stabilization and function in enzyme catalysis and gene regulation. *FASEB J.* **1993**, *7*, 1483–1490. [CrossRef] [PubMed]
35. Castillo-Villanueva, A.; Reyes-Vivas, H.; Oria-Hernández, J. Kinetic stability of the water-forming NADH oxidase from *Giardia lamblia*: Implications for biotechnological processes. *Biotechnol. Biotechnol. Equip.* **2021**, *35*, 1401–1408. [CrossRef]
36. Spencer, P.; Atkinson, T.; Gore, M. The identification of a structurally important cysteine residue in the glycerol dehydrogenase from *Bacillus stearothermophilus*. *Biochim. Biophys. Acta* **1991**, *1073*, 386–393. [CrossRef] [PubMed]
37. Xu, M.Q.; Li, F.L.; Yu, W.Q.; Li, R.F.; Zhang, Y.W. Combined cross-linked enzyme aggregates of glycerol dehydrogenase and NADH oxidase for high efficiency in situ NAD+ regeneration. *Int. J. Biol. Macromol.* **2020**, *144*, 1013–1021. [CrossRef]
38. Ashrafuddin Ahmed, S. The *streptococcal* flavoprotein nadh oxidase I. Evidence linking Nadh oxidase and Nadh peroxidase cysteinyl redox centers. *J. Biol. Chem.* **1989**, *264*, 19856–19863.
39. Silva, P.; Arancibia, V.; Cid, D.; Romero, O.; Illanes, A.; Wilson, L. Catalyst replacement policy on multienzymatic systems: Theoretical study in the one-pot sequential batch production of lactofructose syrup. *Catalysts* **2021**, *11*, 1167. [CrossRef]
40. Lye, G.J.; Woodley, J.M. Application of in situ product-removal techniques to biocatalytic processes. *Trends Biotechnol.* **1999**, *17*, 395–402. [CrossRef]